Laser-Induced Photofragmentation Fluorescence Imaging of Alkali Compounds in Flames

Leffler, Tomas; Brackmann, Christian; Aldén, Marcus; Li, Zhongshan

Published in:
Applied Spectroscopy

DOI:
10.1177/0003702816681010

2017

Document Version:
Peer reviewed version (aka post-print)

Tomas Leffler, Christian Brackmann, Marcus Aldén, Zhongshan Li, Laser-Induced Photofragmentation Fluorescence Imaging of Alkali Compounds in Flames, Applied Spectroscopy (71:6) pp. 1289-1299.

doi: https://doi.org/10.1177/0003702816681010

Laser-Induced Photofragmentation Fluorescence Imaging of Alkali Compounds in Flames

Tomas Leffler[1,2], Christian Brackmann[1*], Marcus Aldén[1], Zhongshan Li[1]

[1]*Division of Combustion Physics, Lund University, Box 118, SE-221 00, Lund, Sweden*

[2]*Vattenfall Research and Development AB, SE-814 26 Älvkarleby, Sweden*

[*]*corresponding author: christian.brackmann@forbrf.lth.se*

INTRODUCTION

Environmental issues and overall efforts to achieve a sustainable energy supply require power plant operators to increasingly consider utilization of a broader variety of biomass sources in the fuel mixture, such as herbaceous material (straw and grass), agricultural by-products (pits, shells and hulls) and municipal waste.[1, 2] However, many of these fuels result in the formation of alkali chlorides such as KCl and NaCl during combustion in power plant boilers. Alkali chlorides are key components for slagging and fouling and they also affect heat-exchange surfaces.[3] In addition, chlorine exposure increases the risk of corrosion on furnace walls, super heaters, and economizers.[4]

Problems related to alkali chlorides can be avoided using fuels with low content of alkali and chlorine, or suppressed by adding sulphur to the process – either by co-combustion with a sulphur-containing fuel or by injection of sulphur-containing additives.[5] Nevertheless, optimum reduction of alkali chlorides requires detailed understanding of the formation process and validation of mechanisms for alkali chemistry, which can be achieved by studies in laboratory flames under well-controlled conditions, see for example Li *et al*.[6] Potassium is the main alkali metal in many biomass fuels[7, 8] and a major component in many of the problems outlined above, thus knowledge on potassium chemistry is highly relevant for proper combustion of biomass fuels.

Laser-based techniques provide non-intrusive probing, in many cases species-specific, with high temporal and spatial resolution for detailed studies of combustion processes. A comprehensive review by Monkhouse[9] summarizes the status up to 2011 of different techniques for online detection of alkali metals in flue gas. Alkali chlorides, such as KCl and NaCl, can be detected by means of photofragmentation fluorescence for which Oldenborg *et al.*[10] used high-power laser pulses in the ultraviolet regime for photodissociation of alkali compounds followed by detection of fluorescence from the excited atomic alkali fragment. Furthermore, Chadwick

et al.[11] investigated photofragmentation fluorescence detection of NaCl and NaOH (sodium hydroxide) using an Excimer laser of wavelength 193 nm for photodissociation and subsequent measurement of Na fluorescence signals at 589 and 819 nm for detection of NaCl and NaOH, respectively. Further investigations of the photofragmentation fluorescence technique have included NaOH detection by multi-photon fragmentation using the 355 nm third-harmonic output from a Nd:YAG laser[12] and studies of collisional quenching of the alkali metal atom fragments.[13]

The photofragmentation fluorescence technique has been applied for detection of alkali compounds in flue gas of Circulating Fluidized Bed (CFB) boilers. Investigations have been made for combustion of coal only[14-16] as well as for co-combustion with biomass with a high content of alkali.[17] Moreover, Erbel *et al*. used the technique in a study of biomass gasification.[18] Sorvajärvi et al. have further developed the technique, combining photofragmentation with absorption measurements of the atomic K fragments for enhanced sensitivity and quantitative concentration measurements.[19, 20] Furthermore, Sorvajärvi et al. have demonstrated this combination for simultaneous measurements of nascent atomic K, KCl, and KOH (potassium hydroxide) employing wavelengths 266 and 320 nm for photofragmentation of KCl and KOH, respectively.[21]

While previous studies include measurements in a single point or averaged along a line, also in practical combustion devices, spatially resolved imaging measurements are also of interest. Employed for detailed studies in laboratory flames such measurements could provide valuable insights for model development and validation. To investigate this approach photofragmentation fluorescence imaging is characterized in this study for detection of KCl and KOH in the post-flame region of premixed laminar methane-air flames seeded with alkali compounds. Investigations include assessment of interferences, comparison of signal levels,

quantification, and estimation of detection limits. Moreover, simultaneous imaging of alkali species is demonstrated for NaCl and KCl in flame.

METHODS

Photofragmentation fluorescence measurements. The experimental set-up for photofragmentation fluorescence, schematically shown in Fig. 1a, contains an ArF Excimer laser (Compex 102, Lambda Physik), which provided pulses at wavelength 193 nm with 25 ns pulse duration and output pulse energy of 50 mJ. For photofragmentation fluorescence measurements the 193 nm laser beam was focused into vertical sheets using different combinations of lenses.

Measurements of photofragmentation fluorescence emission spectra of KCl, KOH, and NaCl were made with the beam focused into a 50 mm sheet using a cylindrical lens of focal length f=300 mm. The fluorescence was collected into a spectrometer (Acton SP-150, grating 300 grooves/mm, Princeton Instruments) using an UV condenser, f=60 mm, and a long-pass filter (WG280, Schott) to suppress scattered laser light. The signals were detected with an intensified CCD camera (PI-MAX I, Princeton Instruments) connected to the spectrometer.

For imaging the detector was instead equipped with an f=50 mm objective (Nikkor f/1.4).

In measurements for quantitative analysis of the photofragmentation fluorescence signal, the 193 nm laser beam was focused using cylindrical lenses of focal lengths f=1000 mm and f=500 mm, which combined with an arrangement of razorblades resulted in a 20 mm vertical sheet. Measurements of potassium species were made using a bandpass filter centred at 766 nm (50 mm dia., OD 4, FWHM 10 nm, Edmund Optics) for detection of K-atom fluorescence and suppression of scattered laser radiation. Simultaneous measurements of KCl and NaCl were made using a stereoscope (Lavision) mounted in front of the objective. Band-pass filters centred

at wavelengths 766 and 589 nm (50 mm dia., OD 4, FWHM 10 nm, Edmund Optics) were inserted in the stereoscope for detection of K- and Na-atom fluorescence signals, respectively.

A burner originally made for atomic absorption spectroscopy (Perkin-Elmer), shown in the photo of Fig. 1b, was used for measurements in alkali-seeded methane-air flames. The burner consists of a spray chamber and a water-cooled head with a central compartment for the premixed fuel-air blend and an outer channel for a co-flow shielding the flame. The diameter of the inner compartment is 23 mm and the head is topped by a circular mesh plate (pore size ~1 mm and length 20 mm). The burner allows for stabilization of flat laminar premixed flames (cf. Fig. 1b). Alkali-seeding is achieved using a nebulizer fed with part of the supplied air, which extracts liquid KCl solution via a sample tube. The KCl solution from the nebulizer is pre-treated in order to have only finer aerosol droplets to pass through the chamber to the burner head whereas larger droplets are removed via a drain tube. Methane and auxiliary air are mixed together with the nebulizer air in the burner's spray chamber to get the total correct fuel-air equivalence ratio (Φ) of the mix.

A nitrogen co-flow of 10 l/min was supplied to the burner head to shield the flame. A steel cylinder (cf. Fig. 1b) was mounted 30 mm above the burner for flame stabilization required for quantitative signal analysis and to be able to make sequential photofragmentation and Rayleigh scattering measurements under steady-state conditions. The total gas flow of air and fuel to the burner was 5.6 l/min and individual flows of nitrogen, air to the nebulizer, primary air, and fuel were controlled by four mass flow controllers with maximum flows of 20, 10, 5 and 1 l/min (Bronkhorst), respectively. Premixed stoichiometric methane-air flames were investigated and the KCl concentration in the seeding solution was varied from 0.01 to 3.0 M.

Rayleigh scattering measurements. The 532 nm second harmonic of a Nd:YAG laser (Brilliant B, Quantel) with a pulse duration of 7 ns and a pulse energy of 120 mJ was used for Rayleigh scattering measurements. The 532 nm beam was aligned into the beam path using a

dichroic mirror, cf. Fig. 1a, and further shaped into a laser sheet of 10 mm height using cylindrical lenses of focal lengths f=-40 mm, f=200 mm, and f=500 mm. A half-wave plate positioned in the beam path was adjusted to achieve vertical polarization for optimal Rayleigh scattering.

Absorption measurements. KCl absorption measurements were made in the flames using the experimental set-up shown in Fig. 1c. UV light from a high-intensity (150 W) UV light source (L1314, Hamamatsu) was radiated through an aperture and collimated using a 90° off-axis parabolic mirror coated with UV-enhanced aluminium and a reflective focal length of f=150 mm (diameter 50 mm, Thorlabs). The collimated UV light beam subsequently passed through another aperture and a plano-convex focusing quartz lens of focal length f=150 mm. After the lens the UV beam passed over the burner top and was reflected five times using UV-enhanced aluminium mirrors (diameter 25.4 mm, Thorlabs) before it was collected in an UV-enhanced collimator (250 - 450 nm, diameter 12 mm beam, SMA, Thorlabs). This construction resulted in a total absorption path length of 138 mm. The collected UV light was then transferred through an optical fibre (FC-UV600-0.5-SR, Azpect Photonics) and subsequently dispersed in a spectrometer (grating 2400 grooves/mm, slit width 50 µm, AVABENCH-75-2048, Azpect Photonics). KCl concentrations were evaluated from the collected spectra by a least-squares fit to a calibration spectrum measured at 860 °C following the procedure presented by Forsberg et al.[22]

Fluorescence data evaluation. Alkali species concentrations have been evaluated from the photofragmentation fluorescence signal, *F*, which can be expressed in emitted photons by Eq. (1)

$$F = \frac{\Omega}{4\pi} l \varepsilon_F A \frac{A_{fi}}{A_{fi} + Q} TN \qquad (1)$$

where Ω is the detection solid angle, *l* the probe volume length, ε_F the detection efficiency for the fluorescence signal, and *A* the probe volume cross section area. The ratio $\frac{A_{fi}}{A_{fi}+Q}$ represents the fluorescence quantum yield where A_{fi} is the Einstein coefficient for spontaneous emission, *Q* the collisional quenching rate, and *T* represents a factor accounting for fluorescence losses due to absorption, so-called trapping. The quantity *N* is the concentration of alkali atoms generated in the excited K-atom 4^2P states by photofragmentation. The fluorescence is obtained from the 4^2P transitions at 766 and 769 nm and the frequencies are $\nu=3.91\cdot10^{14}$ s^{-1} and $\nu=3.89\cdot10^{14}$ s^{-1}, respectively. Assuming that K-atom photofragments are distributed between both the 4^2P states, the average of the coefficient for spontaneous emission for the two transitions can be employed in the evaluation, using values presented by Nandy et al. [23] give $A_{fi}=3.8\cdot10^7$ s^{-1}. Collisional quenching data has been presented by Jenkins[24] and using concentrations of CO, CO_2, O_2, N_2, H_2, and H_2O determined from equilibrium calculations resulted in a total quenching rate of $Q=4.1\cdot10^8$ s^{-1} for a stoichiometric flame. The beam cross section area *A*, is determined by dimensions of the focused laser sheet.

Tuneable diode laser absorption measurements of the potassium D1 line at 769.9 nm were made using a single-mode external cavity laser (DL 100, Toptica Photonics) with output power of 40 mW. The laser was scanned over a frequency range of 25 GHz covering the potassium line and the transmitted laser beam passing through the flame 21 mm above the burner surface was detected by a photodiode (DTE 210, Thorlabs). Analysis of scanned spectra of the K-atom line allowed for determination of potassium atom concentration. The K-atom line shape in the flame was given by a Voigt profile with a Gaussian width of 0.11 cm^{-1} and a Lorenzian width of 0.05 cm^{-1}. An average integrated absorption cross section for the two 4^2P transitions was determined to be $8.36\cdot10^{-6}$ cm^2s^{-1} which distributed over the measured line profile resulted in a peak absorption cross section of $1.6\cdot10^{-11}$ cm^2. Combined with the measured K-atom

concentrations and assuming a path length of 1 cm for passage to the detector in the central region of the flame, the absorption was calculated for the different parts of the K-atom line employing the Beer-Lambert law. Trapping of the photofragmentation fluorescence signal was then calculated by integration over the attenuated line profile.

The quantities related to signal collection and detection efficiency can be retrieved by means of Rayleigh scattering measurements for which the signal, *S*, expressed in number of photons is given by Eq. (2)

$$S = \frac{E_{Rayleigh}}{h\nu_{Rayleigh}} \frac{\partial\sigma}{\partial\Omega} \Omega l \varepsilon_R N_{tot} \qquad (2)$$

In Eq. (2) $E_{Rayleigh}$ is the laser pulse energy for Rayleigh scattering measurements, h Planck's constant, $\nu_{Rayleigh}$ the Rayleigh photon frequency, $\frac{\partial\sigma}{\partial\Omega}$ the differential Rayleigh scattering cross section, ε_R the detection efficiency for the Rayleigh scattering signal, and N_{tot} the total gas number density in the probe volume. The cross section for air at ambient pressure and temperature for wavelength 532 nm is $6.25 \cdot 10^{-32}$ m^2/sr.[25] Using the Rayleigh scattering signal for calibration provides the detection solid angle, Ω, and the probe volume length, l, in the concentration evaluation using Eq. (1). The detector quantum efficiencies are specified to 10% and 3.3% at 532 and 766 nm, respectively. These values together with the transmission, 85%, of the interference filter used for fluorescence detection have been employed for determination of ε_R and ε_F.

In addition, Rayleigh scattering can be utilized for flame temperature measurements by comparison of signals measured in flame and at ambient conditions, taking differences in cross sections into account. For the investigated stoichiometric flame, using Rayleigh scattering cross section data compiled by Zetterberg[26] and major species concentrations determined from chemical equilibrium calculations, the Rayleigh scattering cross section of the product gas in

the post-flame region was found to be a factor of 1.1 higher than that of ambient air. Including this factor in the ratio between Rayleigh signals measured in flame and ambient air allowed for temperature measurements in the flame.

The relation between the concentrations of K atoms, N, and parent species, N_{KCl}, is given by Eq. (3)[27]

$$N = N_{KCl}\Phi(1-e^{\frac{-\sigma E}{h\nu_{laser}A}}) \quad (3)$$

The factor Φ is the yield of photofragments generated from the parent species and is equal to 1 for the investigated case since dissociation of one KCl molecule results in creation of one K atom. Furthermore, σ is the absorption cross section, E the laser pulse energy, and ν_{laser} the laser frequency. Equation (1) can be solved for the concentration of alkali atoms N and the product of Ω and l can be retrieved using Eq. (2). Solving Eq. (3) for N_{KCl} using the obtained value of N in turn allows for evaluation of alkali compound concentrations from the photofragmentation fluorescence data.

RESULTS AND DISCUSSION

Prior to imaging experiments, fluorescence emission spectra were measured to identify potential interferences. Figure 2a shows photofragmentation fluorescence emission spectra measured in stoichiometric flames seeded with KCl (black) and NaCl (grey). Distinct spectral lines from atomic Na and K can be observed at wavelengths 589 and 766 nm, respectively. K-atom fluorescence at 766 nm is also obtained for KOH-seeding as shown in a higher resolution in the spectrum of Fig. 2b, although the line is approximately eight times weaker compared with the case of KCl-seeding. In Fig. 2b the spectrum measured for NaCl seeding also shows a line from Na at 820 nm, also observed previously by Chadwick et al.[11] and mainly attributed to photofragmentation of NaOH formed during combustion. All spectra show fluorescence peaks

at wavelengths 250 – 350 nm, shown in Fig. 2c, mainly attributed to OH radicals generated from photodissociation of H_2O. This could potentially interfere in imaging experiments, but can be removed with suitable filters transmitting the strong contributions of atomic Na and K.

Fluorescence images, averaged over 300 laser pulses, showing photofragmentation fluorescence signals in the product zone of stoichiometric Φ=1.0 methane-air flames are shown in Fig. 3. The images were acquired for seeding with KCl solutions of concentrations 0.5 (a) and 0.01 M (b), and with KOH solution of 0.5 M concentration (c). The images show that signal levels close to the flame front region, located towards the lower image boundary, are low but increase further up in the post-flame region where the major potassium compounds to consider are KCl and KOH. With KCl-seeding, K and Cl elements entering the flame are able to form KCl in the post-flame region. However, via reactions involving water, K atoms are also able to form KOH. Thus, with KCl-seeding flame chemistry allows for formation of both KCl and KOH in the post-flame region, while KOH-seeding merely results in KOH formation. Figure 3d shows a Rayleigh scattering image measured in a stoichiometric flame seeded with 1.0 M KCl solution. The Rayleigh scattering signal of the propagating laser sheet can be seen across the image together with scattered light from the flame stabilizer located above the burner. The lower signal in the hot post-flame region is clearly observed and images of this type have allowed for temperature measurements of the investigated flames. Narrow vertical regions of stronger Rayleigh signal, indicated with arrows, can be observed at the flame edges and is interpreted as scattering from condensed KCl.

Further insights into image interpretation and evaluation can be obtained from profiles of fluorescence signals across the post-flame region. Profiles averaged over a region indicated by the dashed horizontal lines in Fig. 3, covering 13-20 mm above the burner, are plotted in Fig. 4 together with temperature profiles determined by Rayleigh scattering. The fluorescence signal is proportional to gas number density and the profiles have been compensated by multiplication

with the temperature profiles in order to obtain profiles representing relative concentrations. Profiles for the two KCl-seeding concentrations show apparent differences. The 0.5 M KCl-seeding result in maximum signal at the flame edges, cf. Fig. 3a and 4a, where two distinct peaks can be observed. In contrast the image and profile measured for 0.01 M KCl-seeding, cf. Fig. 3b and 4b, shows strong signal across the flame though with some signal decrease at the flame center, as shown in Fig 4b. The major reason for the observed trends is absorption of the fluorescence signal by K atoms formed in the flame chemistry, i.e. fluorescence trapping, during its passage through the flame. This must thus be considered in quantitative evaluation of the flame data, in particular at high seeding levels. Potassium atom levels determined from diode-laser absorption spectroscopy (data not shown) were 1 and 0.02 ppm for 0.5 M and 0.01 M KCl-seeding, respectively. For comparison, broadband UV absorption measurements and evaluation of fluorescence data, discussed in the following, show potassium compound concentrations to be around 10 ppm for the 0.5 M flame and around 0.1 ppm for the 0.01 M flame. For 0.5 M seeding, trapping results in a transmission of the photofragmentation signal to the detector calculated to be 4%. Furthermore, the trapping effect could be confirmed by comparing the signal versus KCl-seeding for the central region of the post-flame region, exhibiting strong trapping, and the edge region where the impact of trapping is lower.

As flame chemistry produces both KOH and KCl, and both of these result in K-atom photofragmentation fluorescence, as shown in Figs. 2 and 3, it is relevant to discuss the contributions of these compounds to the observed signal. Figure 4a also shows a profile measured with 0.5 M KOH-seeding of the stoichiometric flame, corresponding to the image in Fig. 3c. Similar to the KCl profile the KOH profile shows lower signal at the center of the flame where the temperature has reached a stable level around 1470 K. The profiles of KOH and KCl shows signals at the edges that are stronger than the signal at the flame center by a factor of two

and three, respectively. The ratio of the signals generated for KCl- and KOH-seeding is around 2 in the central part of the post-flame region.

The energies required for dissociation and generation of a K-atom fragment in the excited 4^2P state is 5.31 eV and 5.91 eV for KOH and KCl, respectively. While the energy provided by 193 nm photons is insufficient for excitation of K atoms from KCl into higher excited states, dissociation of KOH, requiring less energy than KCl, allows for generation of K-atom fragments in the 5^2S and 3^2D states.[23] Compared with the case of KCl this would introduce additional emission coefficients A_{fi} and collisional quenching rates Q in the fluorescence quantum yield, cf. Eq. 1. Thus, as only the 4^2P emission is detected the photofragmentation fluorescence quantum yield for KOH can be expected to be lower than for KCl.

In addition to the comparison between KCl and KOH presented in Fig. 4a corresponding measurements were made in lean and rich flames of equivalence ratios Φ=0.8 and Φ=1.3. Photofragmentation fluorescence signals for KCl-seeded flames were on average a factor of 2.1 stronger with variations of 15%. From the broadband UV absorption measurements, the 0.5 M KCl-seeding is estimated to generate about 10 ppm KCl in the post-flame region. For this amount of KCl, chemical equilibrium calculations at the measured temperature predicts 6-7 ppm of KOH, i.e. about 40% of the total concentration of KCl and KOH. Diode laser absorption measurements indicated 1 ppm of potassium atoms in the post-flame region for both flames and chemiluminescence measured by the CCD camera also indicated similar K-atom levels for both cases. For the 0.5 M KOH-seeding, without chlorine introduced into the flame, it can thus be expected that ~16 ppm of KOH is formed. Considering this, the photofragmentation fluorescence quantum yield of KOH can be estimated to be around 40% of the yield of KCl. This suggests KCl to be the major signal contribution in the image measured in the KCl-seeded flame for which the temperature is around 1500 K. In the KOH-seeded flame the lack of

chlorine results in more K atoms available for formation of KOH, which becomes the major post-flame potassium compound.

The formation and distribution of KOH and KCl are temperature-dependent which also could affect the shapes of the profiles in Fig. 4. Formation of KCl is reportedly promoted at lower temperature while the formation of KOH is promoted at higher temperature.[6] The larger difference in signal between the edge and the central part of the flame observed for KCl compared with KOH-seeding could also partially be due to enhanced KCl-formation and suppressed KOH-formation in the low-temperature region at the flame edges. In addition, data measured in KCl-seeded flames indicate condensation in the regions of lower temperature at the flame edges. This is demonstrated in the Rayleigh scattering image shown in Fig. 3d, measured in a stoichiometric flame seeded with 1.0 M KCl-solution and showing thin regions of high signal, indicated by arrows, at the flame edges. The enhanced elastic scattering indicates formation of aerosols due to KCl condensation. Calculated vapor pressures using the HSC chemistry software[30] are higher for KOH than for KCl, which then becomes more susceptible to condensation.

Chadwick et al.[11] have shown that it is possible to discriminate between NaCl and NaOH in photofragmentation fluorescence measurements. For both species the photofragmentation process produces Na atoms in the excited 3^2P state, resulting in emission at 589 nm. However, the dissociation energy of NaOH is lower and excess energy is therefore available for further excitation of the Na-atom fragment resulting in additional fluorescence emission for Na, for example at 820 nm as observed in Fig. 2b. As mentioned previously the situation is analogous for the potassium compounds where additional energy available after dissociation of KOH allows for excitation into the 5^2S and 3^2D states.[23] Population of these states would result in fluorescence emission at wavelengths 464, 1174, and 1248 nm. The $3^2D \rightarrow 4^2S$ transition at 464 nm is, however, rather weak with a coefficient for spontaneous emission five orders of

magnitude lower than the $4^2P \rightarrow 4^2S$ transition.[23] The $3^2D \rightarrow 4^2P$ and $3^2D \rightarrow 5^2S$ transitions at 1174 and 1248 nm, respectively, are stronger but are located at wavelengths outside the sensitive range of the employed CCD detector. Thus, implementation of the concept presented by Chadwick et al. would likely be feasible also for KOH using detectors sensitive at near-infrared wavelengths. The energies required for photofragmentation and creation of excited K-atom fragments correspond to threshold wavelengths of 206.8 and 233.1 nm for KCl and KOH, respectively.[10] Thus, a way to induce photofragmentation fluorescence of KOH only, would be to use a laser wavelength longer than 206.8 nm, for which the 213 nm fifth harmonic of a standard Nd:YAG laser could be an appropriate choice. For NaOH photofragmentation Chadwick et al. have also reported on emission from excited OH-radical fragments, attributed to a multiphoton process as the excess energy after photofragmentation is insufficient for OH excitation.[11] In our investigations of KOH, the fluorescence spectra do show OH lines (cf. Fig. 2c), however no difference were observed between spectra measured in KOH-seeded or unseeded flames. A contribution to the OH signal from a KOH multiphoton process is therefore probably much lower than the OH signal obtained from photodissociation of water in the post-flame region.

The photofragmentation process is influenced by the laser fluence according to Eq. (3) and Fig. 5a presents the photofragmentation fluorescence signal versus laser fluence measured in a KCl-seeded stoichiometric methane-air flame. The results indicate an essentially saturated signal with some scatter indicated by the error bars. The saturated process is confirmed in Fig. 5b, which presents results from calculations of the fraction of dissociated KCl and KOH molecules versus laser fluence according to Eq. (3). These calculations include the absorption cross section, which for KCl at 193 nm can be estimated to $3 \cdot 10^{-17}$ cm^2 from data presented by Davidovits and Brodhead.[28] Corresponding data for KOH is, however, not available in literature but following the discussion by Sorvajärvi et al.[21] it can be approximated with that of NaOH

reported by Self and Plane[29] which gives a value of $5.6 \cdot 10^{-18}$ cm^2 at 300 K. The higher cross section of KCl results in a complete dissociation at lower fluence levels than for KOH, which shows a slower increase in the fraction of dissociated molecules. While these calculations indicate that KOH does not fully reach complete dissociation for the experimental conditions with laser pulse energies of around 40 mJ in a focused laser sheet resulting in a fluence of 800 mJ/cm^2, the degree of dissociation is above 90% and both species are considered measured under saturated conditions.

Figure 6a shows the photofragmentation fluorescence signals, measured at the edge (open circles) and center (filled circles) of a stoichiometric flame, versus KCl-seeding. As referred to previously, the signal at the flame edge is directly proportional to the seeding concentration, resulting in a slope close to 1 in Fig. 6a, whereas the signal at the flame center shows a weaker increasing trend with seeding concentration due to fluorescence trapping. Absorption spectroscopy was used to quantify the amount of seeded KCl converted into gas-phase KCl in the flame and post-flame region. Figure 6b shows the KCl-concentrations measured by absorption and photofragmentation fluorescence in the post-flame region of a stoichiometric flame versus KCl-seeding level. Concentrations evaluated from averaged fluorescence data according to Eq. (1), i.e. compensated for fluorescence trapping, for an estimated laser-sheet thickness of 200 µm are in good agreement with results from absorption measurements. Note, that both measurements result in concentrations considerably lower than the KCl-seeding input concentrations of the reactant mixture, plotted on the abscissa, indicating losses of KCl-solution via the burner drain as well as due to precipitation and deposits in the burner system. Quantitative measurements are thus feasible and the accuracy is determined by uncertainties in the quantities of Eq. 1. Uncertainties related to calibration of the signal collection and determination of the laser sheet cross-section area can be minimized and estimated with thorough experimental design. The laser pulse energy for the Rayleigh scattering and the width

of the focused laser sheet can both be determined with accuracies on the order of 5%. The collisional quenching and fluorescence trapping however introduce uncertainties more challenging to assess. Determination of the collisional quenching rate requires knowledge on temperature as well as the concentrations of the major species of the flame and their collisional quenching cross sections. The accuracy of the quenching rate is thus in turn dependent on how accurate these parameters are known, as an example the quenching rate calculated for premixed methane-air flames on the investigated burner configuration varies by 10% for equivalence ratios between Φ=0.8 and Φ=1.3. The fluorescence trapping requires accurate determination of K-atom concentrations, which can be achieved using sensitive absorption techniques. Under the investigated conditions a change in K-atom concentrations of 10% result in a relative change in trapping factor of 5-7%. With experimental uncertainties of these magnitudes the uncertainty of the measured alkali compound concentrations can be estimated to 15-20%.

Imaging measurements are particularly valuable for studies of non-stationary conditions requiring single-shot measurements, exemplified by images measured in KCl- and KOH-seeded flames shown in Fig. 7a and b. The image of KCl (Fig. 7a) has a signal-to-noise ratio of about 300 while for the KOH image (Fig. 7b) it is about 170. The detection limit is, however, determined by the relation between the fluorescence signal and the background radiation from excited K-atoms formed in the flame. An analysis of the detection limit for a signal-to-background ratio of 3 in KCl-seeded flames and an image spatial resolution of 0.7 mm is shown in Fig. 7c. For measurements at post-flame KCl concentrations of a few ppm and data averaged over 300 laser pulses the lower detection limit is on the order of 0.5 ppm. However, for high seeding levels and a higher background of excited K atoms the detection limit instead approaches 3 ppm. Similar analysis for single-shot data shows detection limits of 1 and 5 ppm, respectively, for measured post-flame concentrations. These detection limits, estimated under conditions with a background consisting of alkali emission, are obviously higher than values of

0.1 ppb reported for NaCl and KCl measured in low-background experiments carried out in cells at lower temperatures than in a flame environment.[10, 11]

Figure 8 demonstrates that it is possible to carry out simultaneous single-shot photofragmentation fluorescence measurements of two relevant alkali components: KCl and NaCl, in a fuel mixture within a context of combustion in biomass and waste-fired boilers. The fluorescence image was measured in a flame seeded with a mix of 50% 3 M NaCl and 50% 3 M KCl solution utilizing a stereoscope with band-pass filters for detection of K atoms (766 nm) and Na atoms (589 nm). Signals from K (left, blue) and Na (right, orange) atoms both show a shape mimicking the cone of the flame obtained without the stabilizer mounted above the burner. Even though similar in shape, the signals originate from the two different species without cross-talk between the detection channels, which was confirmed by measurements for seeding of KCl and NaCl separately. Gas-phase KCl and NaCl are detected on the inner part of the cone while stronger signals are obtained on the edges due to lower temperature resulting in higher gas density, enhanced formation of chlorides and possible condensation. While the signals at the edges for the two species are of similar magnitude, KCl shows a signal a factor of ~1.5 stronger inside the cone. The signal is dependent on the concentration N as well as the spontaneous emission coefficient A_{fi} (cf. Eq. 1), which for Na atoms is $1.3 \cdot 10^8$ s^{-1} while the corresponding values for K atoms is $3.8 \cdot 10^7$ s^{-1}.[31, 32] Since signals have been compensated for the detector response at the detection wavelengths, the emission coefficient and the signal ratio suggest KCl concentrations a factor of ~5 higher than NaCl in the post-flame region under this experimental condition.

The presented imaging technique in combination with the earlier findings from Oldenburg et al.[10] and Chadwick et al.[11] can help in the quantifying and visualizing where the different alkali species are formed in the combustion process. Potentially this could be useful in fundamental investigations to characterize co-combustion of coal and biomass fuels containing

sodium and potassium, respectively. The mitigation of alkali-related problems such as high-temperature corrosion, slagging and fouling, that are due to the increased use of biomass fuel of different quality regarding alkali and chlorine[33, 34] demands methods that has the possibility of detecting KCl and NaCl, as demonstrated for this set-up.

CONCLUSIONS

Laser-induced photofragmentation fluorescence can be used for imaging detection of alkali chlorides such as KCl and NaCl and for alkali hydroxides such as KOH with high sensitivity. The application of high-power UV pulses from excimer lasers for photofragmentation allows saturated photodissociation, independent on absorption cross section, to be achieved. Quantitative KCl concentrations up to 20 ppm were evaluated from the fluorescence data and KCl detection limits of 0.5 and 1.0 ppm were determined for averaged and single-shot imaging data, respectively. The method can be employed for detailed studies in laboratory flames to validate chemical kinetic models, and from a fundamental point of view help to increase knowledge and understanding on the fate of alkali-formation from fuel to flue gas in biomass combustion.

ACKNOWLEDGEMENTS

The Swedish Energy Agency, the Knut and Alice Wallenberg foundation through grant KAW2015.0294-ALADIN, the European Research Council (ERC) through Advanced Grant 669466-TUCLA, and Vattenfall AB are gratefully acknowledged for their financial support. The authors would also like to acknowledge the helpful discussions with Joakim Bood and Kajsa Larsson and the support of Qiang Gao for assistance with the diode-laser absorption measurements.

1. H. Balat. "Prospects of biofuels for a sustainable energy future: A critical assessment". Ener Educ Sci Tech-A. 2010. 24(2): 85-111.

2. A. Demirbas. "Potential applications of renewable energy sources, biomass combustion problems in boiler power systems and combustion related environmental issues". Prog Energ Combust. 2005. 31(2): 171-192.

3. S. van Loo and J. Koppejan, The handbook of biomass combustion and co-firing. Earthscan: UK , 2008.

4. H. P. Nielsen, F. J. Frandsen, K. Dam-Johansen, and L. L. Baxter. "The implications of chlorine-associated corrosion on the operation of biomass-fired boilers". Prog Energ Combust. 2000. 26(3): 283-298.

5. H. Kassman, J. Pettersson, B. M. Steenari, and L. E. Åmand. "Two strategies to reduce gaseous KCl and chlorine in deposits during biomass combustion - injection of ammonium sulphate and co-combustion with peat". Fuel Process Technol. 2013. 105: 170-180.

6. B. Li, Z. W. Sun, Z. S. Li, M. Aldén, J. G. Jakobsen, S. Hansen, and P. Glarborg. "Post-flame gas-phase sulfation of potassium chloride". Combust Flame. 2013. 160(5): 959-969.

7. J. N. Knudsen, P. A. Jensen, and K. Dam-Johansen. "Transformation and release to the gas phase of Cl, K, and S during combustion of annual biomass". Energ Fuel. 2004. 18(5): 1385-1399.

8. J. M. Johansen, J. G. Jakobsen, F. J. Frandsen, and P. Glarborg. "Release of K, Cl, and S during Pyrolysis and Combustion of High-Chlorine Biomass". Energ Fuel. 2011. 25(11): 4961-4971.

9. P. Monkhouse. "On-line spectroscopic and spectrometric methods for the determination of metal species in industrial processes". Prog Energ Combust. 2011. 37(2): 125-171.

10. R. C. Oldenborg and S. L. Baughcum. "Photofragment Fluorescence as an Analytical Technique - Application to Gas-Phase Alkali Chlorides". Anal Chem. 1986. 58(7): 1430-1436.

11. B. L. Chadwick, G. Domazetis, and R. J. S. Morrison. "Multiwavelength Monitoring of Photofragment Fluorescence after 193-Nm Photolysis of Nacl and Naoh - Application to Measuring the Sodium Species Released from Coal at High-Temperatures". Anal Chem. 1995. 67(4): 710-716.

12. B. L. Chadwick, P. G. Griffin, and R. J. S. Morrison. "Quantitative detection of gas-phase NaOH using 355-nm multiple-photon absorption and photofragment fluorescence". Applied Spectroscopy. 1997. 51(7): 990-993.

13. K. T. Hartinger, S. Nord, and P. B. Monkhouse. "Quenching of fluorescence from Na(3(2)P) and K(4(2)P) atoms following photodissociation of NaCl and KCl at 193 nm". Appl Phys B-Lasers O. 1997. 64(3): 363-367.

14. U. Gottwald and P. Monkhouse. "Single-port optical access for spectroscopic measurements in industrial flue gas ducts". Appl Phys B-Lasers O. 1999. 69(2): 151-154.

15. U. Gottwald, P. Monkhouse, N. Wulgaris, and B. Bonn. "Simultaneous detection of nickel and potassium in the flue gas of a fluidised bed coal combustor by excimer laser-induced fragmentation fluorescence". Fuel Process Technol. 2003. 80(2): 143-153.

16. P. B. Monkhouse, U. A. Gottwald, K. O. Davidsson, B. Lönn, K. Engvall, and J. B. C. Pettersson. "Phase discrimination of alkali species in PCFB combustion flue gas using simultaneous monitoring by surface ionisation and photofragmentation fluorescence". Fuel. 2003. 82(4): 365-371.

17. M. P. Glazer, N. A. Khan, W. de Jong, H. Spliethoff, H. Schurmann, and P. Monkhouse. "Alkali metals in circulating fluidized bed combustion of biomass and coal: Measurements and chemical equilibrium analysis". Energ Fuel. 2005. 19(5): 1889-1897.

18. C. Erbel, M. Mayerhofer, P. Monkhouse, M. Gaderer, and H. Spliethoff. "Continuous in situ measurements of alkali species in the gasification of biomass". P Combust Inst. 2013. 34: 2331-2338.

19. T. Sorvajärvi, J. Saarela, and J. Toivonen. "Optical detection of potassium chloride vapor using collinear photofragmentation and atomic absorption spectroscopy". Opt Lett. 2012. 37(19): 4011-4013.

20. T. Sorvajärvi and J. Toivonen. "Principles and calibration of collinear photofragmentation and atomic absorption spectroscopy". Appl Phys B-Lasers O. 2014. 115(4): 533-539.

21. T. Sorvajärvi, N. DeMartini, J. Rossi, and J. Toivonen. "In Situ Measurement Technique for Simultaneous Detection of K, KCI, and KOH Vapors Released During Combustion of Solid Biomass Fuel in a Single Particle Reactor". Applied Spectroscopy. 2014. 68(2): 179-184.

22. C. Forsberg, M. Broström, R. Backman, E. Edvardsson, S. Badiei, M. Berg, and H. Kassman. "Principle, calibration, and application of the in situ alkali chloride monitor". Rev Sci Instrum. 2009. 80(2):023104.

23. D. K. Nandy, Y. Singh, B. P. Shah, and B. K. Sahoo. "Transition properties of a potassium atom". Phys Rev A. 2012. 86(5): 1-12.

24. D. R. Jenkins. "Determination of Cross Sections for Quenching of Resonance Radiation of Metal Atoms. 2. Results for Potassium Rubidium and Caesium". Proc R Soc Lon Ser-A. 1968. 303(1475): 453-465.

25. R. B. Miles, W. R. Lempert, and J. N. Forkey. "Laser Rayleigh scattering". Meas Sci Technol. 2001. 12(5): R33-R51.

26. J. Zetterberg. Development of Laser-Spectroscopic Techniques for New Detection Schemes in Combustion Diagnostics. PhD thesis. Lund, Sweden: Lund University, Department of Physics/Combustion Physics, 2008.

27. W. D. Kulatilaka, J. H. Frank, B. D. Patterson, and T. B. Settersten. "Analysis of 205-nm photolytic production of atomic hydrogen in methane flames". Appl Phys B-Lasers O. 2009. 97(1): 227-242.

28. P. Davidovits and D. C. Brodhead. "Ultraviolet Absorption Cross Sections for Alkali Halide Vapors". J Chem Phys. 1967. 46(8): 2968-2973.

29. D. E. Self and J. M. C. Plane. "Absolute photolysis cross-sections for $NaHCO_3$, NaOH, NaO, NaO_2 and NaO_3: implications for sodium chemistry in the upper mesosphere". Phys Chem Chem Phys. 2002. 4(1): 16-23.

30. A. Roine. Outukumpu HSC chemistry for windows version 7.1. Pori, Finland: Outokumpu Research, 2011.

31. J. E. Sansonetti. "Wavelengths, transition probabilities, and energy levels for the spectra of potassium (K I through K XIX)". J Phys Chem Ref Data. 2008. 37(1): 7-96.

32. J. E. Sansonetti. "Wavelengths, Transition Probabilities, and Energy Levels for the Spectra of Sodium (Na I-Na XI)". J Phys Chem Ref Data. 2008. 37(4): 1659-1763.

33. C. J. E. Bajamundi, P. Vainikka, M. Hedman, I. Hyytiainen, J. Silvennoinen, T. Heinanen, R. Taipale, and J. Konttinen. "Towards controlling PCDD/F production in a multi-fuel fired BFB boiler using two sulfur addition strategies. Part I: Experimental campaign and results". Fuel. 2014. 134: 677-687.

34. C. J. E. Bajamundi, P. Vainikka, M. Hedman, J. Silvennoinen, T. Heinanen, R. Taipale, and J. Konttinen. "Searching for a robust strategy for minimizing alkali chlorides in fluidized bed boilers during burning of high SRF-energy-share fuel". Fuel. 2015. 155: 25-36.

Figures

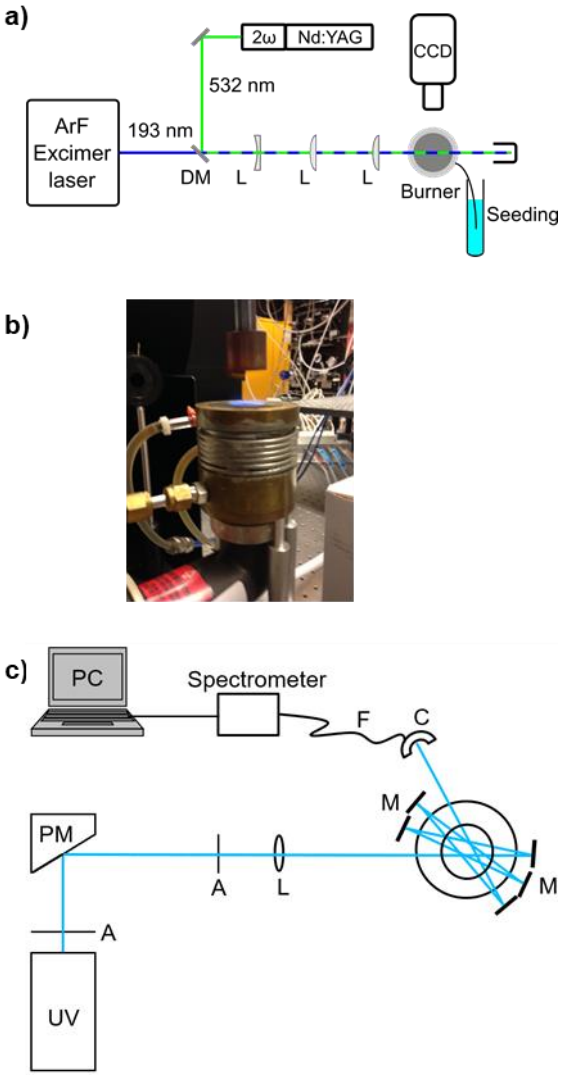

FIG. 1. **a)** Experimental set-up for laser-induced photofragmentation fluorescence and Rayleigh scattering using an ArF Excimer laser and a Nd:YAG laser, emitting wavelengths 193 nm and 532 nm, respectively. DM=Dichroic mirror, L=lenses. Measurements were made in premixed methane-air flames seeded with liquid alkali solution as illustrated to the right in the schematic. **b)** Photo of Perkin-Elmer burner with flat premixed methane-air flame. **c)** Set-up for UV absorption measurements. UV=light source, A=Aperture, PM=Parabolic mirror, L=Plano-convex lens, M=Mirrors, C=collimator, F=optical fibre.

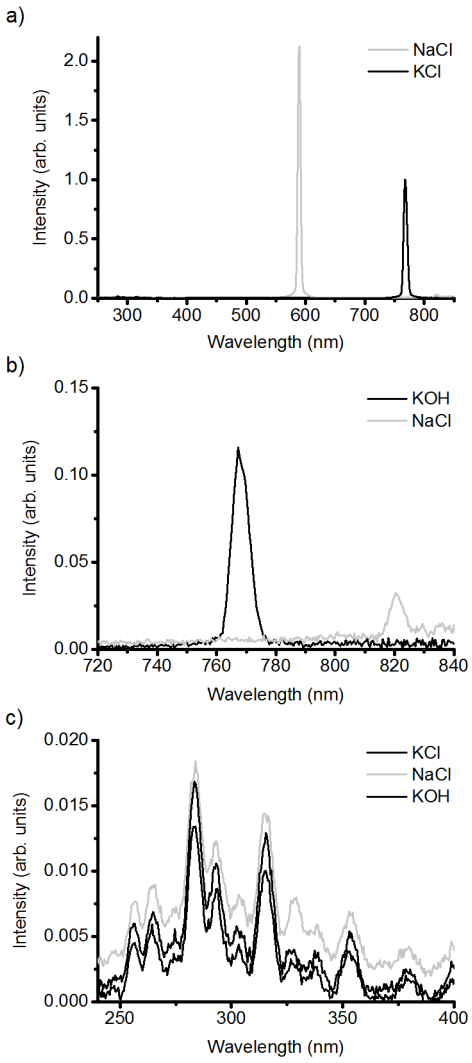

FIG. 2. **a)** Fluorescence emission spectra measured in stoichiometric flame seeded with KCl and NaCl. Spectral lines of atomic K (black) and Na (grey) are observed at 766 and 589 nm, respectively. **b)** Spectrum measured for KOH-seeding (black) shows a K-atom signal ~8 times lower than for KCl-seeding as shown in **a**. The spectrum for NaCl-seeding (grey) shows a line at 820 nm attributed to Na generated by photodissociation of NaOH **c)** Close-up of the spectra for KCl/KOH/NaCl-seeding in the ultraviolet region showing lines attributed to OH radicals of dissociated H_2O.

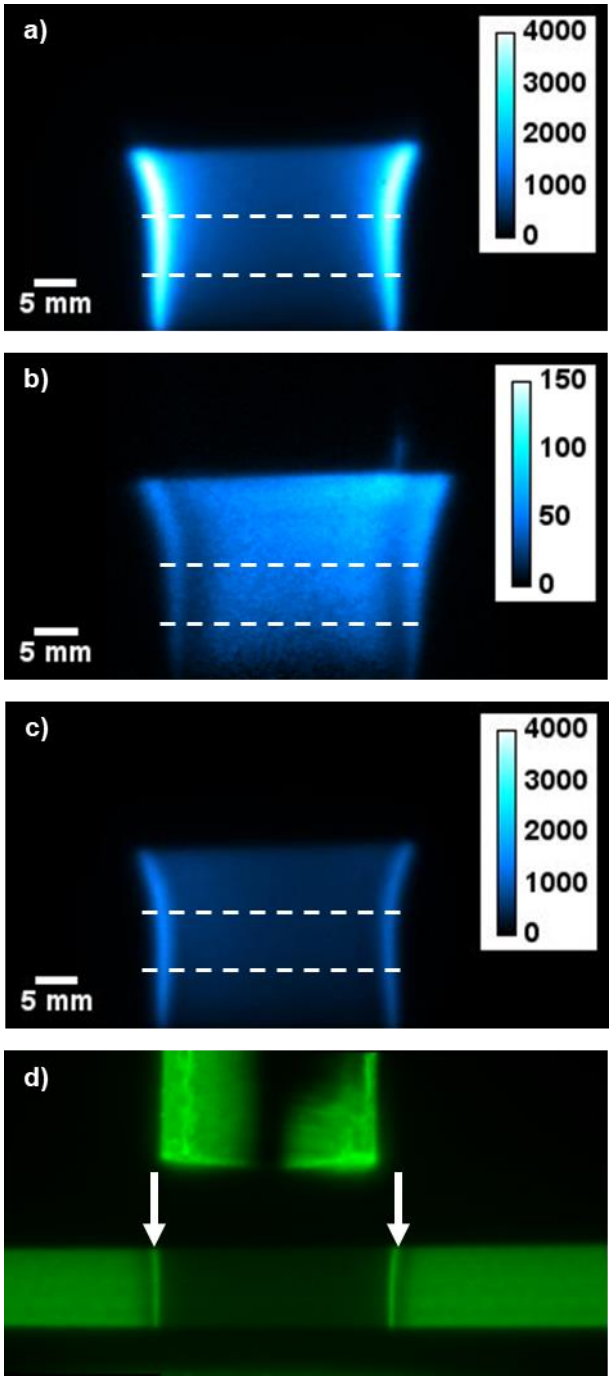

FIG. 3. Averaged (300 frames) photofragmentation fluorescence images measured in premixed methane-air flames of equivalence ratio Φ=1.0 seeded with potassium compounds **a)** 0.5 M KCl **b)** 0.01 M KCl, and **c)** 0.5 M KOH **d)** Rayleigh scattering image measured in KCl-seeded (1.0 M) methane-air flame of Φ=1.0. Narrow regions of high signal at the flame edges, indicated by arrows, suggest KCl condensation. Temperature evaluation from Rayleigh scattering data was made for the regions between the horizontal lines in images a-c.

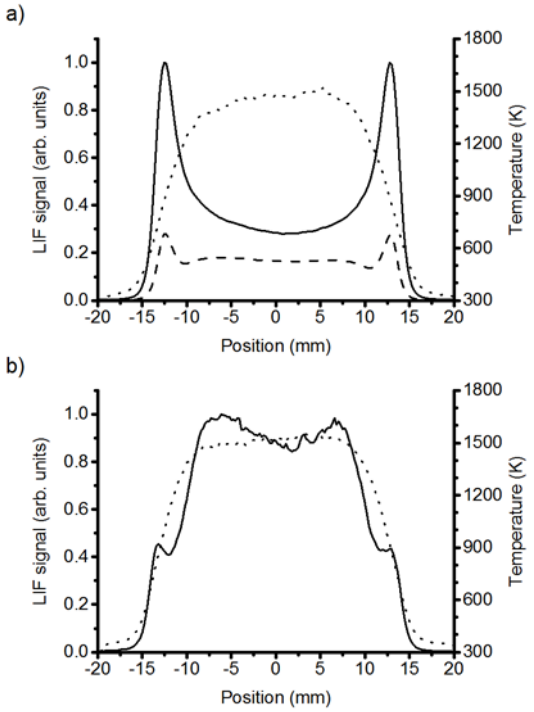

FIG. 4. Temperature (dotted) and alkali compound profiles measured across the post-flame region in stoichiometric methane-air flames a) seeding of 0.5 M KCl (solid) and 0.5 M KOH (dashed) (b) 0.01 M KCl-seeding (solid). High alkali-seeding (a) gives profiles attenuated at the flame center (position 0 mm) due to absorption of the emitted fluorescence. The alkali fluorescence profiles have been compensated for gas number density to obtain profiles representing relative concentrations.

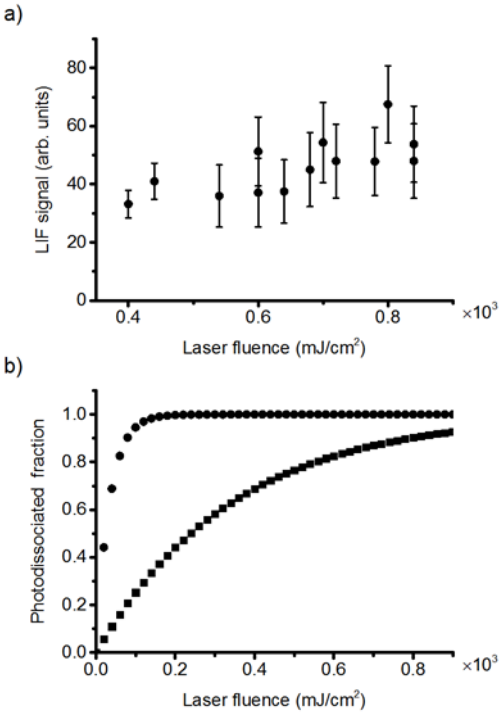

FIG. 5. **a)** Photofragmentation fluorescence signal versus laser fluence measured in a stoichiometric methane-air flame seeded with 0.2 M KCl solution. Each measurement point is an average over 300 laser pulses and the error bars represent the standard deviation. The signal shows an essentially saturated trend. **b)** Calculated fractions of dissociated molecules versus laser fluence for KCl (circles) and KOH (squares). The experimental conditions for flame measurements correspond to ~800 mJ/cm^2, which results in complete dissociation for KCl and strong dissociation for KOH.

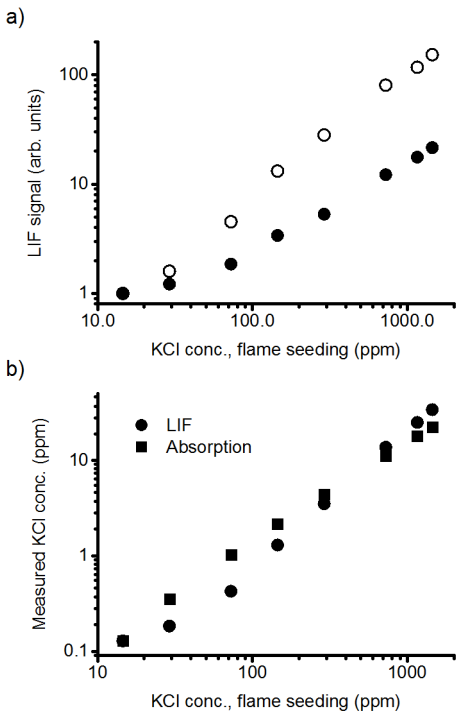

FIG. 6. **a)** Photofragmentation LIF signals versus KCl-seeding concentration in a stoichiometric methane-air flame. The signal measured at the flame boundary (open circles) is directly proportional to the seeding concentration while that measured in the flame center (filled circles) shows a weaker increasing trend due to signal absorption. **b)** KCl concentrations measured by LIF (circles) and UV absorption (squares) versus KCl-seeding concentration in stoichiometric flame.

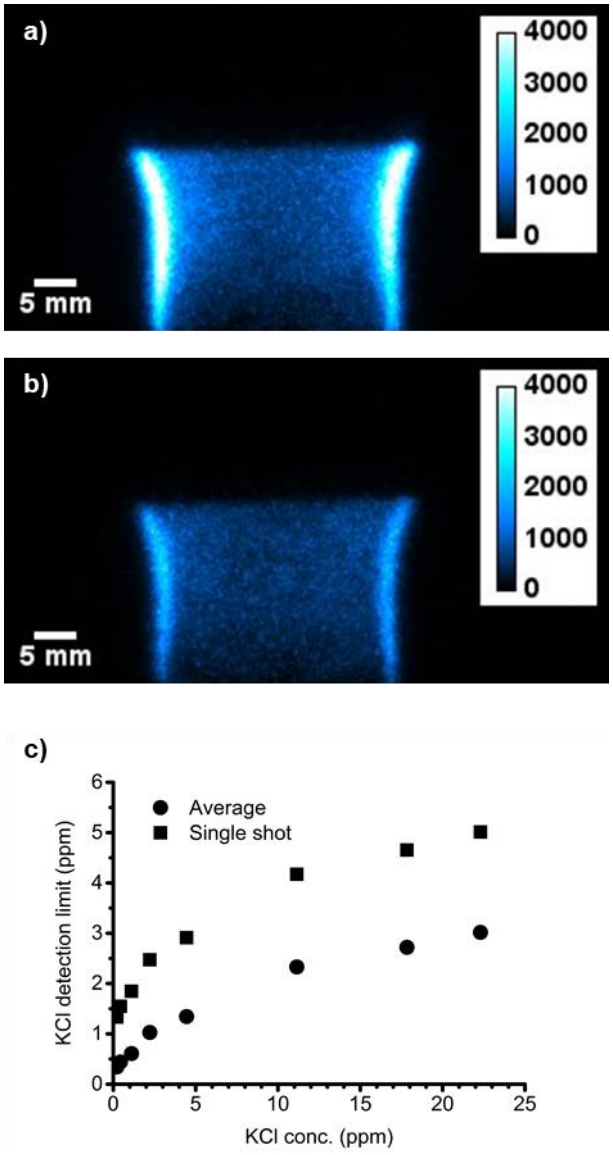

FIG. 7. Single-shot photofragmentation fluorescence images measured in stoichiometric methane-air flames seeded with potassium compounds **a)** 0.5 M KCl **b)** 0.5 M KOH. **c)** Detection limit determined for a signal-to-background ratio of 3 in KCl-seeded flames for images averaged over 300 pulses (circles) and single-shot images (squares).

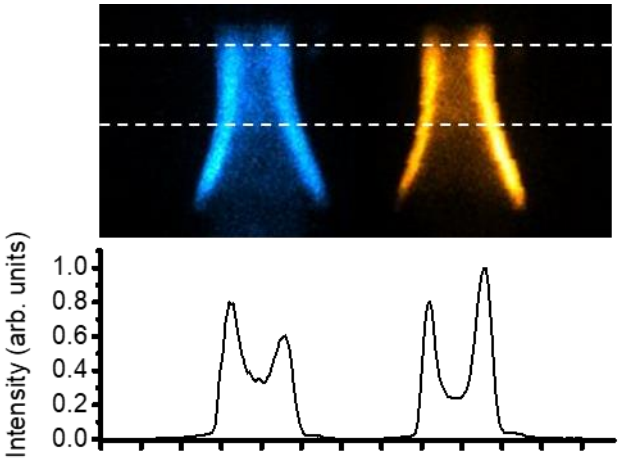

FIG. 8. Fluorescence image (top) with signals from K (left) and Na (right) atoms measured simultaneously using a stereoscope in a stoichiometric premixed methane-air flame with 1.5 M KCl-/NaCl-seeding. An intensity profile, integrated over the region between the horizontal white lines, is shown below.